International Journal of WILDLAND FIRE

Development and validation of fuel height models for terrestrial lidar—RxCADRE 2012

Journal:	*International Journal of Wildland Fire*
Manuscript ID:	WF14170
Manuscript Type:	Research Paper
Date Submitted by the Author:	18-Sep-2014
Complete List of Authors:	Rowell, Eric; University of Montana, Department of Forest Management; University of Montana, National Center for Landscape Fire Analysis Seielstad, Carl; University of Montana, National Center for Landscape Fire Analysis Ottmar, Roger; USDA Forest Service, Pacific Northwest Research Station
Keyword:	Fuel, Fuel: availability, Fuel: classification, Remote sensing, Fire management: proscribed

Development and validation of fuel height models for terrestrial lidar—RxCADRE 2012

Eric M. Rowell[A,B,D], *Carl A. Seielstad*[A,B], *and Roger D. Ottmar*[C]

[A]National Center for Landscape Fire Analysis, The University of Montana, 32 Campus Drive, Missoula, MT 59812, USA

[B]Department of Forest Management, College of Forestry and Conservation, The University of Montana, 32 Campus Drive, Missoula, MT 59812, USA

[C]US Forest Service, Pacific Wildland Fire Sciences Lab, 400 N 34th Street, Suite 201, Seattle, WA 98103, USA

[D]Corresponding author. Email: eric.rowell@firecenter.umt.edu

Summary

We discuss the efficacy of terrestrial laser scanning for collecting continuous measurements of grass and shrub fuelbeds in the northwestern Florida as part of the 2012 RxCADRE experiments. Spatial bias is examined, resulting in fuel height data that correspond closely with field measurements of height.

Abstract

Terrestrial laser scanning (TLS) was used to collect spatially continuous measurements of fuelbed characteristics across the plots and burn blocks of the 2012 RxCADRE experiments in Florida. Fuelbeds were scanned obliquely from plot/block edges at a height of 20 m above ground. Highly instrumented plots (HIPs) were scanned at ~8 mm spot spacing from a single viewing position pre- and postfire while blocks were scanned from six perspectives prefire and four postfire at ~2 cm spot spacing. After processing, fuel height models were developed at one meter spatial resolution in burn blocks and 0.5 m resolution in plots and compared with field measurements of height. Spatial bias was also examined. The resultant fuel height data correspond closely with field measurements of height and exhibit low spatial bias. They show that field measurements of fuel height from field plots are not representative of the burn blocks as a whole. A translation of fuel height distributions to specific fuel attributes will be necessary to maximize the utility of the data for fire modeling.

Keywords

Terrestrial laser scanner, grass fuels, shrub fuels, TLS-based height metrics, spatially explicit, prescribed fire, fuels characterization

Introduction

Fire science and management typically utilize statistical inference and generalization to produce fuels data for fire behavior prediction (Anderson 1982; Burgan and Rothermel 1984; Keane 2013). The emergence of next-generation wildland fire behavior models that simulate fire propagation through 3-dimensional lattices at fine grain has placed new demands on fuels data (Linn *et al.* 2002; Morvan and Dupuy 2004; Mell *et al.* 2007; Pickett *et al*. 2009; Prince *et al.* 2010). However, distributing fuel realistically across landscapes is difficult, and measuring three-dimensional locations of fuels in the field accurately is time consuming and hard to replicate. Consequently, most fuels data are collected within small areas (transects or plots) and must be abstracted to represent fuels on larger domains. Given the very high spatial variability observed in even fairly simple fuelbeds (Keane *et al*. 2012), the need to describe the actual arrangement of materials as an alternative to abstraction has increased irrespective of domain size. Further, because fuelbeds used in validation of fire behavior prediction cannot be disturbed by field sampling before burning, a remote sensing approach is required.

Recent advances in laser scanning are producing more replicable and accurate renderings of fuels in regards to the spatial distribution of plant elements. Experiments in the southeastern United States have integrated terrestrial laser scanning (TLS) to extract volumes of shrub fuels in laboratory experiments (Loudermilk *et al.* 2009), as well as to fuse TLS data with thermal images of fire behavior in long-leaf pine forests (Hiers *et al.* 2009). Outside of the realm of fuels, experiments to detail plant area density as a function of voxel-based canopy volume in wheat, shrubs and trees (Hosoi and Omasa 2006; Van der Zande *et al.* 2006; Hosoi and Omasa 2009) have yielded strong correlations with dry biomass.

In each of these instances there is a requirement for high spatial resolution data and measurements from multiple perspectives to reduce occlusion from foreground objects and to maximize penetration into vegetation (Hosoi and Omasa 2009). These previous approaches show promise for characterizing individual plant elements in controlled environments, but the characterization of fuels matrices over larger domains in natural environments using TLS data has not been widely investigated. Given considerable uncertainties in estimating specific fuels attributes such as mass by size-class or surface area to volume ratio, the potential near-term advantage of TLS for providing improved fuels data is in mapping characteristics of the fuelbed in terms of the height, shape, and arrangement of vegetation across landscapes up to a few hectares in size with the purpose of explicitly characterizing some of the spatial variability in fuels that may affect fire behavior and effects.

This paper describes methods for acquiring and processing high resolution TLS data across 0.04 ha-plots and 2-ha blocks of mixed grass and shrub fuels in the southeastern United States as developed through the Prescribed Fire Combustion and Atmospheric Dynamics Research Experiment (RxCADRE) conducted at Eglin Air Force Base, Florida. Data accuracy and bias are quantified in the 2-ha blocks where scans were collected from 10 perspectives per block (40 individual scans). Data from the 0.04-ha plots are not presented in this paper due to simple collection modes (one overhead perspective per plot) and precedent analysis presented in Rowell and Seielstad (2012). We report accuracies associated with the spatial fidelity of the complex acquisition modes of TLS data and hypothesize that the majority the error within the point clouds is introduced as a function of how the laser samples objects at the farthest ranges from scan origin. We also speculate that variability between height metrics from TLS and field measurement are the result of characterization modes and not spatial incongruities that cascade from the processing stream. This research shows how integration of large TLS point clouds can be used to produce spatially explicit and continuous measurements of fuelbed height over 2-ha areas at ~2 cm resolution, in conjunction with the other measurements of RxCADRE described in this issue.

Methods

Study area

Terrestrial laser scanning (TLS) data were acquired at Eglin Air Force Base, Florida, in October 2012. Eglin AFB is located in the panhandle of northwestern Florida, USA, which was originally a unit of the former Choctawhatchee National Forest; Eglin is an important resource in the management of longleaf pine ecosystems with 180,000 ha of longleaf pine sandhills and flatwoods (for site map and details see Ottmar *et al.* in this issue). Landscapes with dimensions of 100 m x 200 m (S blocks) were established in two fuel types, grass-dominated and shrub-dominated, and were subsequently burned with strip head fires. Additionally, 20 m x 20 m plots (highly instrumented plots) (HIPs) were established in large operational prescribed burn blocks of either longleaf pine forest or non-forest that are frequently burned with prescribed fires. These blocks and HIPs form the basis for fuels measurement using TLS.

Field data

One meter square clip plots were measured adjacent to each TLS sampling area (Ottmar *et al.* in this issue). For the six S-blocks, one square meter preburn plots (n=25 per block) were established around the perimeter of each 2 ha area at 20-m intervals. Each field plot was monumented with a metal pole on its southeast corner. Plots on the eastern edge of each block were offset eastward by one meter so they did not fall within the burn block itself. Metal poles were wrapped with retro-reflective tape for easy identification within the TLS point cloud. Small field plots in the nine HIPs were monumented identically to the S-blocks. Nonforested HIPs field plots were 0.25 m^2 (n=9 per HIPs) and equally spaced by five meters on three sides of the HIPs. The upwind side of each HIP was unsampled to allow for fire to enter unimpeded by disturbance of the fuelbed. Field measurements for all small field plots included maximum height, average "center of mass" height, canopy cover, and dry biomass weight by lifeform (grass, forb, and shrub). Plots were also photographed obliquely from the north to document prefire spatial organization of fuel elements.

TLS data collection and processing

Laser scans were completed pre-and postburn using an Optech ILRIS™ 3_6D-HD instrument scanning at 10 kHz. Two modes of data were captured for the RxCADRE project: first, the six S-blocks representing relatively homogeneous and continuous grass fuels interspersed with shrubs over 100 m x 200 m extents (block S9 is not included in these analyses as there were issues related to acquisition of the data including too small of a view window that ultimately excluded the reflective poles used to tie scans together.). Details of the RxCADRE sample design are reported by Ottmar *et al.* (this issue). TLS sampling protocols for the HIP plots were set up to capture overhead representations of fuelbeds at ~8 mm spot spacing. The laser was mounted in an articulating boom lift and raised to a height of 20 m above ground with a downward viewing tilt angle of 45°. The scanner was operated from the ground using a tablet computer with a wireless connection. At full extension of the boom lift, the scanhead was positioned 9 m, horizontally, from plot edge. A single scan captured the entire plot. For instances in forested

HIPs, data were collected from 3 to 7 perspectives at variable heights to minimize occlusion of the fuelbed by tree boles and canopies.

In the S-blocks, the TLS instrument was also positioned in the mobile boom lift at a height of 20 m above the fuelbed. Laser scans were collected at six positions around each burn block (Fig. 1) at 20-m horizontal distance from the edge of the block. Postfire scans were collected from the east and west positions only for a total of four per block. In each scan, the laser was pointed downward at an angle of 23°. Scanner settings were optimized to achieve consistent point density across the block with the caveat that point density necessarily declines as range increases. The ILRIS laser allows point density to be set as a function of focal distance; all S-block scans were set to collect 2-cm spot spacing at 90 m, ranging from 8 mm at 20-m range to 56 mm at 300-m range. Time-of-flight scanners collect richer datasets near the point of origin of the scan with less dense point spacing as range increases. As the laser pulse moves away from the ILRIS instrument, the point spacing increases linearly with range at a rate of 16.8 mm per 100 m of range. Additionally, the illuminated footprint of the scanner increases linearly with range, becoming less sensitive to canopy gaps as spot size increases (Seielstad *et al*. 2011). Spot size in the foreground of each S-block was 16 mm, expanding to 29 mm at 100 m range.

TLS processing

Each scan was initially corrected to a GPS control data set (as collected in the RxCADRE experiment) around each block using the Polyworks software suite (Innovmetric: Quebec, Canada) by replacing corner post locations in the raw point clouds with GPS locations. The ILRIS laser scanner collects data in individual 40° x 40° windows which then need to be aligned with one another. Scan-to-scan corrections were completed by selecting identifiable points within the control data (usually monument posts) and then further refining the scan correction using the automated align algorithm within Polyworks. The corner reference points were more easily identified in postburn scans; therefore these points were used to tie adjacent scan scenes together to create a reference for the preburn scans. Because all laser scans were collected from the same locations, pre- and postburn, preburn scans were aligned by using the locations of the postburn scan head as the initial control points. Matching of scans was highly dependent on the auto-align algorithm in Polyworks. The absence of hard targets in the prefire scans made matching of scenes difficult. Polyworks uses a proprietary meshing algorithm in the auto-align procedure. In dispersed fuelbeds, the meshing algorithm struggles to manifest identifiable objects such as the corner posts in enough detail to accurately merge scans. Therefore, an open-source point alignment software package was employed to refine alignment (Cloud Compare 2014) using individual points rather than meshes. All scans from each scanhead location were merged together using the TLS processor (developed in the lead author's lab and written in IDL), and adjacent scan groups were aligned to the group showing the least variability in alignment quality and encompassing the greatest number of visible metal posts. Scan groups were aligned and merged by selecting coincident points and applying an alignment matrix to orient each group into a common projected space. All scan groups were then merged into a single dataset for each burn block and clipped to a 20-m buffer around each burn block. These block datasets were then converted into lidar-specific .las format files and an initial surface and ground separation was performed within LASTools (rapidlasso GmbH, Gilching, Germany) using the LASGround algorithm.

Initial assessment of the ground surface classification suggested differential occlusion of ground points within the center of the burn blocks compared to edges (e.g. 'ground' returns within the fuel height model [FHM] appear lifted in block centers compared with areas at the edges where ground is clearly identified and separate from the FHM). We suggest that occlusion as a function of oblique viewing angles preferentially samples upper reaches of the fuels canopy with less representation of lower fuel objects and the ground. To correct for this condition, airborne scanning laser (ALS) data (for methods see Hudak *et al.* in this issue) collected at the same time as the TLS data were used to adjust the TLS data for geoid and normalized height using the TLS Processor DTM Correct routine written in IDL. This routine imports .las format laser data and interpolates the ALS ground points into a bare earth digital terrain model (DTM), in this case, at 0.5 m^2 resolution. The bare earth TLS data points were compared to the coincident ALS ground points and differences between elevations were used to adjust the TLS data to the proper geoid height for both ground and FHM strata. Corrected geoid heights for the FHM were then differenced from the digital elevation model (DEM) to produce the normalized heights above ground.

TLS data accuracy assessment

Vertical and horizontal accuracy of TLS data were assessed on three criteria. To assess accuracy, point clouds from each of the small field plots were extracted by importing feature datasets of the TLS point clouds into the ArcGIS environment and identifying highly reflective lidar points (intensity values >8000). These reflective data points generally represent low gain returns from the highly reflective retro-tape encasing the 1-m tall aluminum poles at each field plot corner. The points representing monumented plot corners were isolated by selecting 1 m x 1 m buffers around clusters of highly reflective points. At each corner post, 1 m^2 plot boundaries representing the field plots were digitized using the plot corner as the southeast corner of the field plot. Points from monumented plot corners were cleaned to remove reflective artifacts such as ghosting (Seielstad *et al.* 2011) and remaining points were spatially joined with the field plot locations identified above. The result was a cleaned FHM for each small field plot.

The first level of assessment regards the horizontal accuracy of scan-to-scan representations of the corner posts. Plot corner points from each scan station were compared to all coincident corner points for each 2 ha block, with associated errors reported as root mean square error (RMSE). Each plot corner was assessed in the horizontal and vertical domain. The second level of assessment regards vertical error from scan station to scan station. For all combinations of scan stations for each 2 ha block, 0.5 m^2 resolution bare earth DEMs were extracted using the BLAST2DEM routine in LASTools lidar processing suite. These DEMs were imported into the ArcGIS environment, where raster calculations were conducted and zonal statistics based on the clip plots extracted. The third level of assessment regards spatial bias between plot corners as determined by the comparison of TLS derived post locations with surveyed GPS points.

Spatial bias

To assess variability of height metrics as a function of distance from scan station, height-normalized laser data were clipped to block boundaries and examined as a function of distance from block centroids. We hypothesized that as scan distance increases towards the center of the block, the increasingly oblique nature of the scan could result in differential occlusion of ground, thus skewing the fuel height model higher in the center of the plot. In effect, viewing vertically-oriented grass fuels from above may reduce the probability of detecting foliage, particularly at top of canopy, compared with viewing them obliquely. A smaller laser spot size may produce a similar effect. Testing this hypothesis we examined height metrics in 10-m wide concentric rings centered on block centroids out to 50 m distance (block edges on east and west sides).

TLS-based height metrics

Height metrics were extracted from the height distribution of each 1 m^2 field plot including mean height, standard deviation height, inflection height, and the first and second peak of the distribution (Fig. 2). The first peak of the height distribution is the highest frequency height bin (from bottom) greater 1 cm in height. The second peak is the second highest frequency after the first peak. Two mean height metrics were calculated; the first mean height uses all points in the plot subset and the second mean excludes all points that are ≤1 cm to reduce the influence of the ground points on the average. The inflection point is calculated by using a derivative function on the frequency values of the histogram. The function outputs signed values of the slope of the histogram and looks for a sign change to positive for heights 5 cm greater than the height of the first peak. This inflection point is hypothesized to represent the transition from grass clumps, low forbs, and shrubs to grass seed heads and taller shrubs. In previous work, the inflection height of grass fuel matrices was systematically lower than inflection heights associated with shrub fuels (Rowell and Seielstad 2012). Aside from vector based height metrics, raster based height metrics were generated across each S-block using LASCanopy in the LASTools suite. These products included maximum, mean, minimum, standard deviation, first, fifth, tenth, twenty fifth, fiftieth, seventy fifth, ninetieth, ninety fifth, and ninety ninth percentile heights at one meter spatial resolution.

Results

Horizontal and vertical accuracy of plot corner posts

For these results, accuracies are derived through comparison of highly reflective points around plot corners. The horizontal accuracy assessment (Table 1) produces average between-scan easting and northing errors for all posts of 10.75 mm and 9.94 mm, respectively. For individual blocks, S5 contained that largest latitudinal error of 13.97 mm and S4 had the largest longitudinal error (11.43 mm). The vertical accuracy assessment results in between-scan errors ranging from 40 to 120 mm. Assessment of the vertical accuracy of the segmented plot corners indicated better alignment between adjacent scans in blocks S3, S4, and S5. Blocks S7 and S8 exhibited larger error indicating less certainty regarding alignment of some adjacent scan stations. The latter blocks exhibited larger magnitude vertical error suggesting less certainty in definition of ground between some scan stations, though there may be some other effect resulting from the more heterogeneous fuelbed that might occlude tops of the poles from being accurately sampled from all directions.

Vertical error from bare-earth assessment

These results summarize the vertical accuracies in regards to scan-to-scan comparisons of bare earth interpolated surfaces. The vertical offsets derived from scan-to-scan comparison of bare earth interpolated surfaces (Table 1) produced average error of 8.83 mm across all S-blocks. Lowest vertical errors were associated with block S3 (5.41 mm) and highest vertical errors were associated with block S8 (15.84 mm). Given the between-scan consistency of bare earth surfaces, the differences in vertical accuracy obtained from bare earth points versus plot corner posts (from above) are likely attributable to the difficulty in characterizing post heights consistently at long scan distances.

Comparison with GPS control points

Comparison of 35 GPS surveyed points (6 to 8 per block) with the predicted points from the TLS data showed offsets for all blocks (Table 2) ranging from 75 to 185 cm. Error was systematic in S3 and S4 but less so in the other blocks. Subtle error in 1 to 2 individual scan stations in each block was evident in S4–S8. After a second-order polynomial transform, RMSE was reduced to less than a millimeter for S3 and S4, and to 14 to 19 cm for S5–S8. The internal consistency of the untransformed point clouds was high as evidenced by coincidence of posts in the aligned scans. The observed offsets from the GPS survey points shows that the internal alignments of the point clouds did not perfectly align with the surveyed geometry. It is probably not coincidental that the largest error occurs in shrub-dominated plots where identification of posts in the point clouds is more difficult.

Height of vegetation

Maximum heights of field-collected and TLS derived data were compared to assess the ability to predict heights of fuel elements. These results show a reasonable relationship between maximum heights of both datasets ($r^2 = 0.70$, adjusted $r^2 = 0.70$, $p<0.0001$) (Fig. 3). The scatter plot of maximum heights reveals general agreement between the dependent and independent observations at heights of ≥50 cm. Below this threshold, there is more variability in the estimated maximum height and the laser tends to overpredict (bias of 9.6 cm). For instances of over prediction, these results appear to be caused by contamination of the plot point clouds due to ghosting from the reflective corner posts and subtle misalignment of plot boundaries due to uncertainty of the corner point used to anchor each 1-m^2 plot polygon. Where TLS derived maximum height is underestimating the maximum height substantially (4 cases), plot misalignment is the primary culprit.

Very weak relationships were observed between TLS mean height and field-estimated center of mass height (not shown) and it is not evident that relationships should exist given how field estimation was executed. However, variability in scan angle might be expected to produce variations in characterizations of central tendency particularly in vertically-oriented fuels such as grasses. However, no consistent spatial bias is evident for maximum or mean heights (Table 3) as characterized by trends in means from center of blocks to edges. In grass-dominated S4 and S5, heights declined by 4 cm on average from centroid to edge, but this effect is not apparent in grass-dominated S3. In shrub-dominated S7 and S8, small changes between distance rings from centroid are random. Overall, the average absolute difference in maximum heights between rings is 4.8 cm with negative and positive values equally represented. Variability as characterized by standard deviation of heights is very consistent across all blocks.

While these data don't absolutely resolve the question of spatial bias, they suggest that bias, if present, is small. Additional evidence supporting the conclusion of no bias can be found in comparison of maximum height data from coincident field and TLS measurements and from all maximum height data from each block (Table 4). As noted above, TLS and field heights track consistently for the small field plots with overestimation by TLS. Comparison of these results with TLS-derived maximum heights for entire blocks suggests that fuels are consistently taller on average across the blocks than indicated by either field or TLS measurements from the small field plots. Though there was significant trampling of the fuelbeds outside of the clip plots, care was given to not disturb the clip plots before TLS scanning. To further examine whether proximity of the small plots to scan stations (overhead perspectives, small spot sizes) contributed to these differences, block boundaries were buffered by 10 m inward and then maximum height metrics were recomputed for these areas. Maximum heights were no different along block edges than across entire blocks, suggesting consistent height characterization across the blocks and supporting the conclusion that the field plots are not representative of the blocks with respect to canopy top.

Further assessment of the fuel height model for 1-m wide transects at the 100 m or halfway north-south mark on 2 ha blocks (S4, S5, S7) shows mean height trending lower for the grass dominated blocks (S4, S5) and higher for the shrub dominated blocks (S7) (Figs. 4*a*, 4*b*). There also appears to be a more rapid reduction in sampling frequency for shrub- and oak-dominated blocks (S7) with point counts dropping over 50% within 15m of the scan origin. The latter effect is almost certainly attributable to occlusion.

Discussion

Before this study, it was not evident that consistent measurements of fuel heights across domains >1 ha were practical from TLS. Potential error associated with stitching together many scenes of diffuse vegetation combined with instability of the scanning platform was unknown. Further, the inherent variability in scan angle, spot size, and density across the blocks raised questions of data consistency. Intuitively, one might anticipate that as scan angle becomes more oblique, the laser may tend to sample higher in the fuelbed especially in vertically oriented fuels such as grasses. As spot size increases, the amount of detected canopy gap should decrease, potentially reducing characterization of elements lower in the fuelbed. It is more difficult to speculate on the impacts of variations in data density. However, data density varied by a factor of five across the S-blocks, but never declined below 100 returns m^{-2}.

Despite these uncertainties, the geometric consistency of scans from the S-blocks appears high and there is little evidence for spatial bias, perhaps because scan angles and spot sizes are effectively mixed at any point on the landscape. Canopy top (maximum height) is measured consistently as evidenced by comparisons with field data and by examining heights as a function of distance from block centers. The TLS does overpredict height in the small field plots, but the measurements also suggest that the fuelbeds are consistently taller across the blocks than the field measurements. In short, the TLS appears to provide an improved spatially explicit representation of fuel height within the blocks.

The validity of other TLS height metrics such as mean and standard deviation is unknown due to the absence of similar field measurements, although each of the TLS metrics appears spatially consistent across the blocks. The inability to match laser height distributions with similar field measurements is a chronic problem in lidar remote sensing. In this study, maximum height is the only viable field validation metric obtained. We believe that direct reconciliation of TLS height measurements with field measured heights other than the maximum height will likely be unsuccessful. Therefore, developing models to translate lidar height metrics to specific fuels metrics will be necessary. A useful target starting point for modeling is biomass prediction because field plot measurements of biomass are unequivocal. However, given the typical importance of a canopy cover metric in lidar biomass prediction combined with the difficulty in producing consistent cover metrics from oblique TLS scans, there remains considerable uncertainty for using TLS to predict attributes such as fuel load. Initial investigation with scan data from the more richly-sampled HIPs plots showed that the surface area of meshed point clouds correlated well with prefire fuel mass, although the approach did not work well in the S-blocks. In the latter areas, reduced data density produced mesh volumes with artificially inflated surface areas due to excessively large triangulated facets. The application of convex hulls and mesh surface areas to fuel load estimation is the subject of ongoing research.

Perhaps the most promising area of future work is developing fuel type classifications from laser height metrics (e.g. shrub, grass, and bare). Preliminary application of unsupervised classification techniques (ISODATA; Principal Components) reveals coherent spatial pattern that is difficult to interpret with available field data due to the mixture of vegetation types within validation plots. It may be that comparisons of pre- and postfire laser height metrics with spatially explicit fire energy measurements from airborne and ground-based thermal radiometers will aid in understanding some of the observed variations in TLS height metrics in mixed fuels.

With respect to field sampling and processing techniques, this research identified useful protocols as well as shortcomings. Extensive monumenting with retro-reflective tape (used on highway signs) was critical for establishing geometry and for closely identifying locations of field plots. Conversely, the 50 cm aluminum boxes used to monument block corners were not useful for stitching scans together because they were not resolved in enough detail from the farthest scan stations to provide consistent tie points. A consideration when using the reflective tape was the contamination of plots with ghost points as described in Seielstad *et al.* (2011), which contributes strongly to the TLS height bias observed in the field plots. Ghosting occurs when areas of high reflectance are averaged with a background of lower reflectance objects creating a trailing cloud from the highly reflective surface towards the background. These erroneous data were mostly removed from the validation datasets by thresholding intensity although residual points remained which artificially inflated maximum height estimated from the TLS data, specifically in sites dominated by taller grasses. The prevalence of mixed fuelbeds combined with imperfect field plot identification in the scans also resulted in sloppy height comparisons where tall fuels occurred along field plot edges. Scanning from the boom lift provided a stable platform except when winds exceeded ~6 m sec^{-1}, but controlling the scanner remotely was also very important in maximizing stability. For processing TLS data from natural landscapes, software that renders individual points rather than meshes is important for identifying specific targets such as monument poles. For validation purposes, future projects would benefit from field plots distributed within the burn units, at least some plots established in homogenous fuels, and direct field measurements of monumented pole heights.

Without the DEM corrections derived from the airborne laser altimeter, vegetation in the center of the blocks would be biased downward in height because the ground surface is not as well characterized when all scan angles are highly oblique and data density is relatively low. Further, the availability of high-quality GPS ground control allowed precise spatial reconciliation of the lidar data with other data collected. These caveats highlight the uniqueness of the multidisciplinary approach afforded by RxCADRE, and point to the difficulties (and cost) in obtaining quality datasets. All of the TLS scans for RxCADRE were completed in four full-time weeks of effort by a field crew of three, and processing of data to the point reported in this paper was completed in about six months of full-time work and much trial-and-error by two analysts. Although efficiencies have been gained that can be applied to future acquisitions, it should be acknowledged that TLS is not necessarily an alternative to field measurements of fuels in terms of time savings.

Finally, although the height data produced in this study are not yet widely applicable to fire modeling, it is worth considering how they might be used for that purpose. The canopy top metric (maximum height) defines the volume occupied by fuel at one meter spatial resolution. Canopy top alone does not address how much fuel resides in the volume, where it is concentrated, or what its characteristics are. However, we anticipate that height of maximum amplitude, inflection points, or central tendency metrics will address where biomass is concentrated in the vertical domain. The big unknown is how much fuel exists in a given cell. Fuel loading will need to be modeled from the height distributions or fuel types will have to be classified so that fuel characteristics can be inferred from field measurements. In the meantime, it would be worth investigating model sensitivity to fuels variability to determine how accurate the fuels data need to be.

Conclusion

This study marks an approach in which surface fuels heights are characterized across 2-ha burn blocks that are relatively big by TLS standards. The resultant fuel height data correspond with field measurements of height and are spatially accurate. They represent a first step toward spatially explicit and continuous fuels data for fire modeling. They can be represented at multiple scales and resolutions and are potentially useable for many types of modeling. The translation of height data to fuel attributes is the subject of current and future research. Ultimately, the utility of TLS-derived fuels for modeling largely relies on success of the latter endeavor.

Acknowledgements

This research was funded by the Joint Fire Science Program (Project #11-2-1-11), with additional support from the National Center for Landscape Fire Analysis. We thank the Pacific Northwest Research Station for fuels data collection (Joe Restaino, Clint Wright, and Jon Dvorak) and Kevin Hiers and Brett Williams for logistical support at Eglin Air Force Base.

References

Anderson HE (1982) Aids to determining fuel models for estimating fire behavior. USDA Forest Service, Intermountain Forest and Range Experiment Station, General Technical Report INT-122. (Ogden, Utah)

Burgan RE; Rothermel RC (1984) BEHAVE: fire behavior prediction and fuel modeling system— FUEL subsystem. USDA Forest Service, Intermountain Range and Experiment Station, General Technical Report INT-167. (Ogden, UT)

CloudCompare. 2014. CloudCompare: 3D point cloud and mesh processing software: open source project. http://www.cloudcompare.org.

Hiers JK, O'Brien JJ, Mitchell RJ, Grego JM, Loudermilk EL (2009) The wildland fuel cell concept: an approach to characterize fine-scale variation in fuels and fire in frequently burned longleaf pine forests. *International Journal of Wildland Fire* **18**, 315–325. doi: 10.1071/WF08084

Hosoi F, Omasa K (2006) Voxel-based 3-D modeling of individual trees for estimating leaf area density using high-resolution portable scanning lidar. *IEEE Transactions on Geoscience and Remote Sensing* **44**, 3610–3618. doi: 10.1109/TGRS.2006.881743

Hosoi F, Omasa K (2007) Factors contributing to accuracy in the estimation woody canopy leaf area density profile using 3D portable lidar imaging. *Journal of Experimental Botany* **58**, 3463–3473. doi: 10.1093/jxb/erm203

Hosoi F, Omasa K (2009) Estimating vertical plant area density profile and growth parameters of a wheat canopy at different growth stages using three-dimensional portable lidar imaging. *ISPRS Journal of Photogrammetry and Remote Sensing* **64**, 151–158. doi: 10.1016/j.isprsjprs.2008.09.003

Keane RE (2013) Describing wildland surface fuel loading for fire management: a review of approaches, methods and systems. *International Journal of Wildland Fire* **22**, 51–62. doi: 10.1071/WF11139

Keane RE, Gray K, Bacciu V (2012) Spatial variability of wildland fuel characteristics in northern Rocky Mountain ecosystems. USDA Forest Service, Rocky Mountain Research Station, Research Paper RMRS-RP-98. (Fort Collins, CO)

Linn R, Reisner J, Colman JJ,Winterkamp J (2002) Studying wildfire behavior using FIRETEC. *International Journal ofWildland Fire* **11**, 233–246. doi:10.1071/WF02007.

Loudermilk EL, Hiers JK, O'Brien JJ, Mitchell RJ, Singhania A, Fernandez JC, Cropper WP, Slatton KC (2009) Ground-based LIDAR: a novel approach to quantify fine-scale fuelbed characteristics. *International Journal of Wildland Fire* **18**, pp 676–685. doi: 10/1071/WF7138

Mell W, Jenkins MA, Gould J, Cheny P (2007) A physics based approach to modeling grassland fires. *International Journal of Wildand Fire* **16**, 1–22. doi: 10.1071/WF06002

Morvan D, Dupuy JL (2004) Modeling the propagation of a wildfire through a Mediterranean shrub using a multiphase formulation. *Combustion and Flame* **138**, 199–210. doi: 10/1016/j.combustflame.2004.05.001

Ottmar et al. (this issue)

Pickett BM, Isackson C, Wunder R, Fletcher TH, Butler BW, Weise DR (2009) Flame interactions and burning characteristics of two live leaf samples. *International Journal of Wildland Fire* **18**, 865–874. doi: 10.1071/WF08143

Prince DR, Anderson BT, Cole WJ, Dennis M, Fletcher TH (2010) Modeling a burning shrub with and without wind using a semi-empirical model. Poster. Association of Wildland Fire 3rd Fire Behavior and Fuels Conference, Spokane, Washington (October 25-29, 2010).

Rowell E, Seielstad C (2012) Characterizing grass, litter, and shrub fuels in longleaf pine forest pre- and post-fire using terrestrial lidar. Proceedings. In: Proceedings of Silvilaser 2012, Vancouver, BC, Canada.

Seielstad C, Stonesifer C, Rowell E, Queen L (2011) Deriving fuel mass by size class in Douglas-fir (*Pseudotsuga menziesii*) using terrestrial laser scanning. *Remote Sensing* **3**, 1691–1709. doi: 10.3390/rs3081691

Van der Zande D, Hoet W, Jonckheere I, Van Aardt J, Coppin P (2006) Influence of measurement set-up of ground-based LiDAR for derivation of tree structure. *Agricultural and Forest Meteorology* **141**, 147–160. doi: 10.1016/j.agrformet.2006.09.007

Fig. 1. (*a*) An example of the fuelbed for block S3 from the boom lift, (*b*) TLS data clipped to the block boundary with scan locations, and (*c*) a three-dimensional graph demonstrating height variability for a 10 m x 10 m subset of the TLS data.

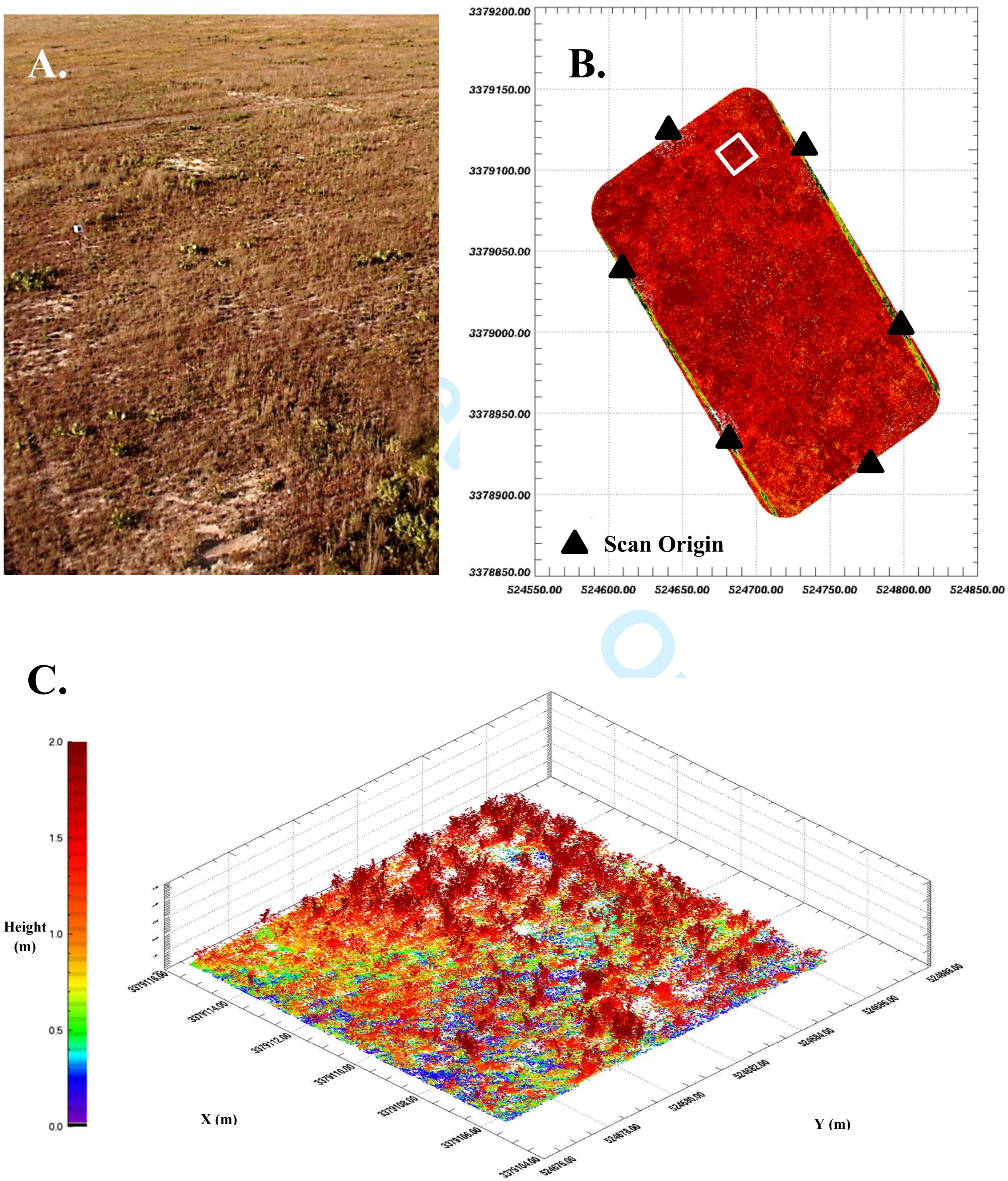

Fig. 2. (*a*) An example of a normalized histogram of the TLS fuel height distribution with the peak frequency, mean height, inflection point, and second peak frequency for plot 18 in block S4, and (*b*) the plot photo of the same area.

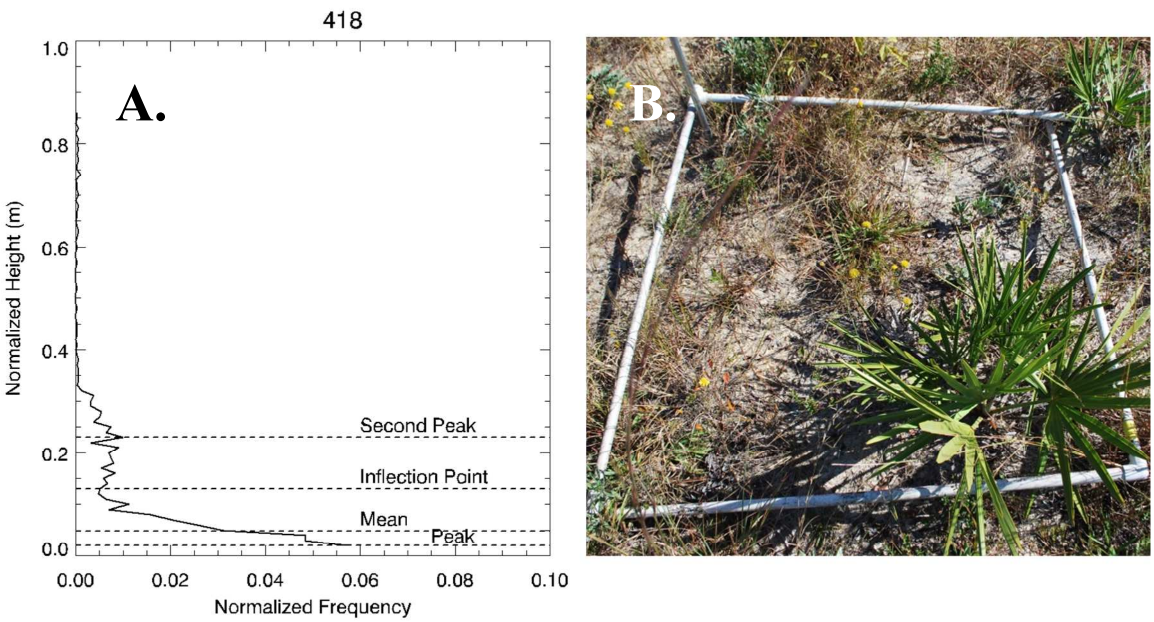

Fig. 3. Scatter plot of observed and TLS-based maximum height for clip plots in the S-blocks demonstrating the overestimation of height from the TLS estimate.

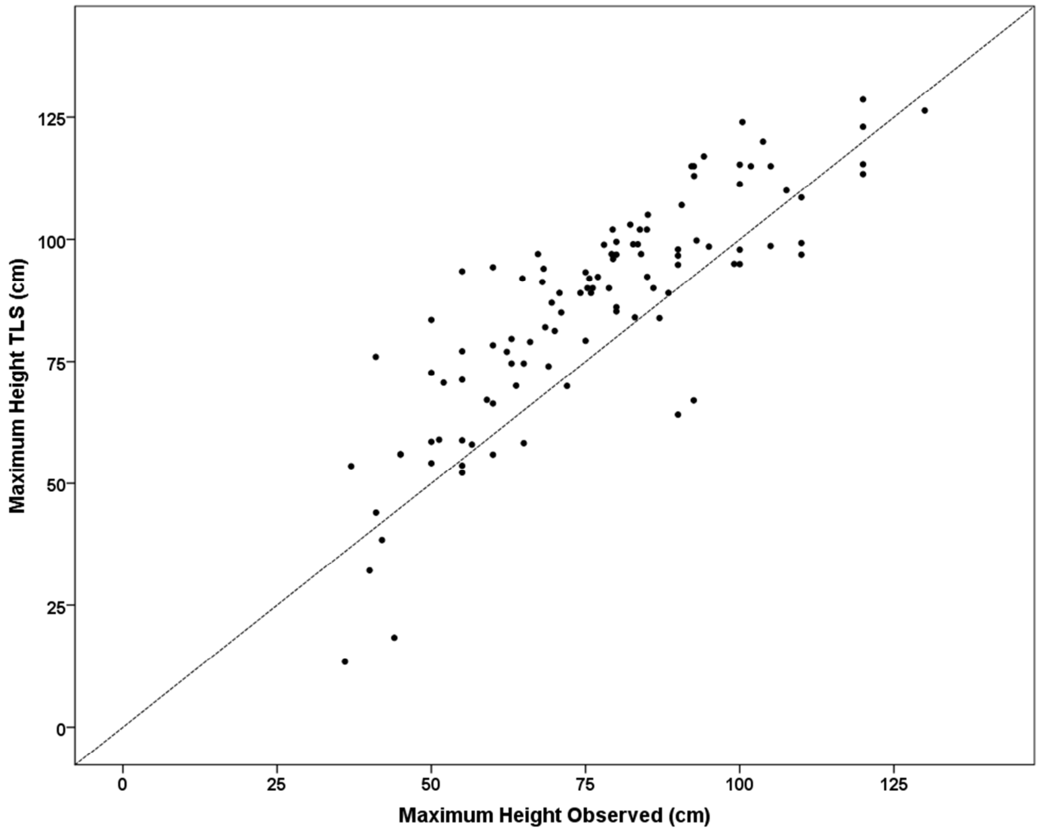

Fig. 4. A sample of three 1-m wide transects from the origin of a scan across to the origin of the opposing scan with the running maximum height (dashed line) and the running mean height (solid line). (*a*) The top two transects are from S3, the bottom transect is from S7. (*b*) Graphs depicting the number of TLS points as a function of range, where the highest density is on either end of the graph near the origin of the scans.

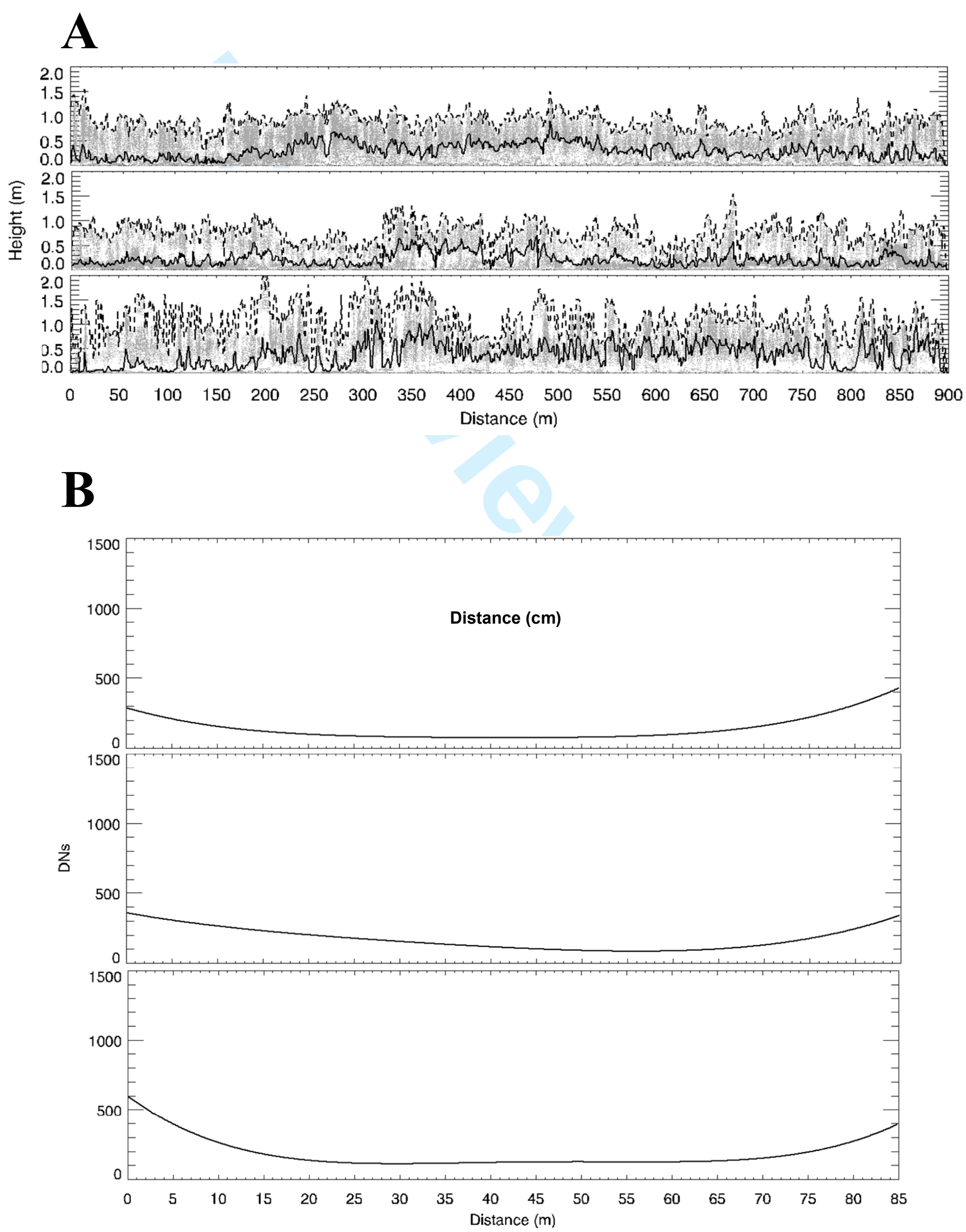

Table 1. Scan to scan errors associated with the merging of opposing scans into a single dataset

Errors are reported as root mean square error (RMSE) for horizontal and vertical domains representing identified plot corners in the point cloud. The vertical RMSE is for the bare earth is the RMSE of the difference for each scan direction compared to all other scans in a block.

Block ID	Plot posts error (cm)			Bare earth vertical error (mm)
	X	**Y**	**Z**	
S3	0.1	0.1	5.9	5.4
S4	0.1	0.1	5.3	6.8
S5	0.1	0.9	3.9	6.8
S7	3.0	2.0	11.0	6.1
S8	3.0	4.0	12.1	15.0

Table 2. Differences between TLS post locations and GPS survey points before and after 2nd-order polynomial transformation

Root mean square error for TLS and GPS data pre- and post- second-order polynomial transformation

Block ID	Root mean square error	
	Pre-transform (cm)	Post-transform (cm)
S3	74.9	<0.01
S4	97.8	<0.01
S5	147.0	14.5
S7	74.0	18.5
S8	185.0	19.3

Table 3. Reported maximum, mean, and standard deviation height for doughnuts of TLS normalized height data at 10-m increments from the centroid of each S-block

Block ID	Height (cm)	Distance from plot centroid				
		0–10 m	10–20 m	20–30 m	30–40 m	40–50 m
S3	max	0.89 ± 0.17	0.91 ± 0.17	0.96 ± 0.17	0.96 ± 0.18	0.94 ± 0.19
	mean	0.39 ± 0.07	0.40 ± 0.08	0.42 ± 0.08	0.43 ± 0.08	0.41 ± 0.10
	stddev	0.17 ± 0.04	0.18 ± 0.04	0.20 ± 0.04	0.20 ± 0.04	0.20 ± 0.04
S4	max	0.89 ± 0.21	0.99 ± 0.20	0.95 ± 0.21	0.92 ± 0.23	0.89 ± 0.23
	mean	0.36 ± 0.11	0.40 ± 0.13	0.38 ± 0.12	0.35 ± 0.13	0.29 ± 0.12
	stddev	0.21 ± 0.05	0.22 ± 0.04	0.22 ± 0.05	0.22 ± 0.06	0.22 ± 0.07
S5	max	0.96 ± 0.18	0.98 ± 0.21	0.98 ± 0.20	0.95 ± 0.20	0.87 ± 0.20
	mean	0.38 ± 0.09	0.41 ± 0.12	0.41 ± 0.13	0.38 ± 0.11	0.31 ± 0.10
	stddev	0.21 ± 0.04	0.22 ± 0.05	0.22 ± 0.05	0.22 ± 0.05	0.20 ± 0.05
S7	max	1.20 ± 0.23	1.12 ± 0.26	1.04 ± 0.26	1.06 ± 0.27	1.09 ± 0.25
	mean	0.53 ± 0.15	0.48 ± 0.16	0.43 ± 0.15	0.43 ± 0.16	0.43 ± 0.16
	stddev	0.28 ± 0.07	0.26 ± 0.07	0.24 ± 0.07	0.25 ± 0.08	0.26 ± 0.08
S8	max	0.95 ± 0.23	0.92 ± 0.25	0.96 ± 0.23	0.96 ± 0.26	0.97 ± 0.25
	mean	0.33 ± 0.11	0.30 ± 0.12	0.31 ± 0.11	0.30 ± 0.13	0.30 ± 0.12
	stddev	0.22 ± 0.06	0.22 ± 0.07	0.23 ± 0.07	0.23 ± 0.07	0.24 ± 0.07

Table 4. Reported mean maximum, and standard deviation height for clip plots collected around the block for TLS normalized height data and the mean maximum height for each block

Block	Field plot height (cm)		TLS plot height (cm)		Block total TLS height (cm)	
	Max	Stdev	Max	Stdev	Max	Stdev
S3	74.72	21.63	80.24	24.10	93.0	20.0
S4	76.32	24.97	77.84	24.64	91.0	22.0
S5	68.36	25.89	72.48	20.80	92.0	21.0
S7	79.40	26.50	89.00	18.52	1.07	26.0
S8	**86.64**	**30.01**	**96.01**	**18.13**	**97.0**	**28.0**